XLVI CILAMCE
VITÓRIA - ES - BRAZIL - 2025
XLVI IBERO-LATIN AMERICAN CONGRESS ON COMPUTATIONAL METHODS IN ENGENEERING

Comparison of Continuum Models in the Numerical Simulation of the Nonlinear Behavior of Concrete

Luccas Silva[1], Roque Pitangueira[1], Lapo Gori[1], Leandro Silva[1], Pamela Reges[1]

[1]*Dept. of Structures (DEES), Federal University of Minas Gerais (UFMG)*
Av. Antônio Carlos, 6627 - Escola de Engenharia - Bloco 1 - 4o andar, sala 4215, Pampulha, Belo Horizonte - MG - CEP 31270-90
luccas-fsilva@ufmg.br, roquepitangueira@gmail.com, lapo@ufmg.br, leandro@dees.ufmg.br, pamelanogueira@ufmg.br

Abstract. Concrete is a widely used material in civil engineering, characterized by its high heterogeneity, as it is composed of a cement paste and aggregates of varying shapes, sizes, and properties. This complex composition makes it difficult to accurately represent its behavior using classical solid mechanics models. Traditionally, structural analysis considers behavior based on the classical continuum model, also known as the Cauchy continuum, which simplifies the material as being composed of infinitesimal points. However, this approach may not be sufficient to faithfully represent materials with complex microstructures, such as concrete. In this context, generalized continuum models have emerged, such as the micropolar continuum, also known as Cosserat. These models take into account the existence of microstructures with non-negligible dimensions, allowing each point in the material to have additional degrees of freedom, such as independent rotations and internal deformations. This formulation enables a more accurate representation of scale effects and local discontinuities. The present work aims to numerically simulate the nonlinear behavior of the same structure using the formulations of the two aforementioned continuum types, in order to compare the analysis efficiency, computational cost involved, and the accuracy of the results obtained. It is expected that the micropolar model will require greater computational effort but will provide results that are more consistent with reality, especially when considering the heterogeneity of concrete, which is not adequately represented by the simplifications of the classical continuum.

Keywords: Concrete; Cauchy Continuum; Micropolar Continuum; Nonlinear Behavior

1 Introduction

The Finite Element Method (FEM) is one of the most widely used numerical tools for nonlinear structural analysis, being extensively applied in both academic research and industrial practice [1]. Its formulation enables the investigation of complex phenomena in various engineering fields, such as subsea pipelines [2], bridges [3], concrete fracture [4], and slope stability [5].

The accuracy of FEM simulations strongly depends on the constitutive modeling, grounded in Continuum Mechanics, which describes material behavior under loading. Among the existing formulations, the classical Cauchy continuum and the Cosserat micropolar continuum stand out. The latter introduces independent rotational degrees of freedom, allowing for the representation of phenomena not captured by the classical theory, such as size effects and microrotations [6, 7].

This work aims to compare FEM-based responses using Cauchy and Cosserat formulations in nonlinear structural problems, assessing the influence of the adopted theory on the results. The main contribution is to identify scenarios where micropolar models may provide more realistic predictions, supporting future research on fracture analysis and heterogeneous materials.

The paper is organized as follows: (i) introduction; (ii) theoretical background, summarizing the adopted formulations; (iii) methodology, detailing the simulated examples and software; (iv) results and discussion; and (v) conclusions.

2 Theoretical background

2.1 Cauchy continuum

The Cauchy continuum, illustrated in Figure 1, is formulated under the assumption that the body consists of infinitesimal material points with negligible dimensions. In the analysis of the transformation between the initial undeformed configuration (X) and the deformed configuration (x), rigid body motion of these points is disregarded, thereby simplifying the governing equations.

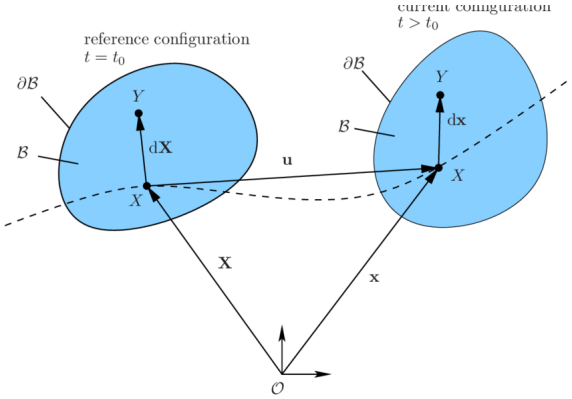


Figure 1. Physical representation of the Cauchy continuum, adapted from Ralf [8].

The formulation presented by Mal and Singh (1991) [9] allows the computation of strains (ϵ) from prescribed displacements (u), as given in Eq. 1, and subsequently the Cauchy stress tensor (σ) through Eq. 2, where λ and μ are the Lamé constants [9], and δ_{ij} denotes the Kronecker delta. Furthermore, stresses and strains must satisfy the equilibrium and compatibility conditions expressed in Eqs. 3 and 4, where f_i represents the body forces.

$$\epsilon_{ij} = \frac{1}{2}[\nabla u_{ij} + (\nabla u_{ij})^T] \tag{1}$$

$$\sigma_{ij} = \lambda \epsilon_{kk} \delta_{ij} + 2\mu \epsilon_{ij} \tag{2}$$

$$\sigma_{ji,j} + f_i = 0 \tag{3}$$

$$\epsilon_{ij,km} + \epsilon_{km,ij} - \epsilon_{ik,jm} - \epsilon_{jm,ik} = 0 \tag{4}$$

For analyses involving large deformations, the use of the Cauchy tensor alone is insufficient to accurately describe the stress state, requiring the introduction of the first Piola–Kirchhoff tensor ($\overline{\sigma}$) and the second Piola–Kirchhoff tensor ($\widetilde{\sigma}$). These are related to the Cauchy stress tensor by Eqs. 5 and 6, where J denotes the deformation Jacobian and F the deformation gradient.

$$\overline{\sigma} = J {F_{ij}}^{-1} \sigma_{ij} \tag{5}$$

$$\widetilde{\sigma} = J G_{ij} \sigma_{ij} {F_{ij}}^{-T} \tag{6}$$

The constitutive equations relating the stress tensor to the strain tensor are expressed in Eq. 7. This relationship is defined by the fourth-order elastic tensor (c), which incorporates material properties through the elastic

modulus (E) and Poisson's ratio (ν). Owing to the stress equilibrium equation (Eq. 3), the elastic tensor must satisfy the symmetry conditions presented in Eq. 8. Additional details on the classical theory can be found in Mal and Singh (1991) [9].

$$\sigma_{ij} = c_{ijkm}\epsilon_{km} \tag{7}$$

$$c_{ijkm} = c_{jikm} = c_{ijmk} = c_{mkij} \tag{8}$$

2.2 Cosserat continuum

As previously mentioned, the classical continuum assumes that the body is composed of infinitesimal material points, and therefore of negligible dimensions. However, when dealing with heterogeneous media, such as reinforced concrete, this assumption may compromise the accuracy of the results, since the material heterogeneity is neglected [10].

Conversely, the Cosserat continuum considers the body to be formed by particles with non-negligible dimensions (Q) and (q), as illustrated in Figure 2. This model accounts for moments that produce microrotations of these particles, adding additional rotational degrees of freedom [11] to the Cauchy continuum, thereby improving the analysis of heterogeneous materials.

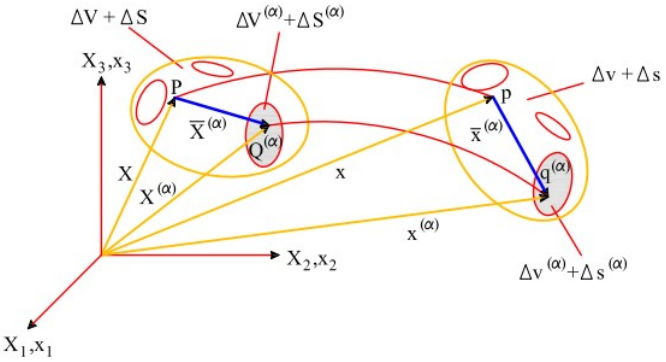


Figure 2. Physical representation of the Cosserat continuum, adapted from Fuina [11].

Microrotation is characterized by the tensor (ϕ_k), which defines two new quantities in addition to the strain described in Eq. 1: (γ_{ij}) and (κ_{ij}), as expressed in Eqs. 9 and 10, respectively. These quantities are related to variations in dimensions and curvatures of the microstructure.

$$\gamma_{ij} = u_{j,i} - \epsilon_{ijk}\phi_k \tag{9}$$

$$\kappa_{ij} = \phi_{j,i} \tag{10}$$

Regarding the constitutive relations, in addition to those already presented in the classical continuum, the strain energy density (U_0) is now a function of γ_{ij} and κ_{ij}, as established in Eqs. 11 and 12. The solution of the problem depends on the boundary conditions [11]. Thus, in addition to the stress equilibrium equation (Eq. 3), the governing equation for microrotations must also be satisfied, as expressed in Eq. 13, where l_i represents the prescribed body moment.

$$\sigma_{ij} = \frac{\partial U_0}{\partial \gamma_{ij}} \tag{11}$$

$$\mu_{ij} = \frac{\partial U_0}{\partial \kappa_{ij}} \tag{12}$$

$$\mu_{ji,j} + \epsilon_{ijk}\sigma_{jk} + l_i = 0 \tag{13}$$

It is observed that the Cosserat continuum constitutes an extension of the classical continuum, such that, when the additional assumptions are disregarded, the equations reduce to those of Cauchy. Further details on this formulation can be found in Fuina (2009) [11].

3 Methodology

The analyzed structure consists of an L-shaped panel, as illustrated in Figure 3, subjected to a vertically distributed load applied along its lateral edge. The model was idealized under the plane strain assumption, with a thickness of 100 mm. The material was considered as linear elastic and isotropic, with an elastic modulus of 25,850 N/mm² and a Poisson's ratio of 0.18.

The simulations were carried out using the INSANE software [12], developed at the Federal University of Minas Gerais (UFMG). This computational environment employs the Finite Element Method (FEM) and supports nonlinear analyses using different formulations of Continuum Mechanics.

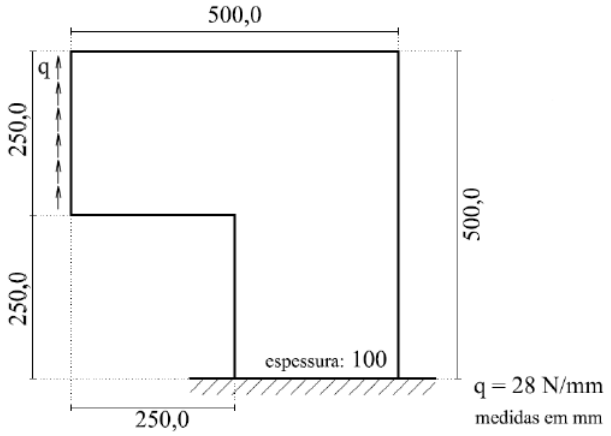


Figure 3. L-shaped panel model, adapted from INSANE [13].

The numerical model was discretized into 48 quadrilateral Q8 elements, with full integration (3×3 Gauss points). Boundary conditions were defined with full displacement constraints (Dx = Dy = 0) along the base of the panel. The applied load consisted of a set of vertically distributed nodal forces on the panel's lateral edge. The loading was applied incrementally, with an initial load factor of 0.02, using the Generalized Displacement Control method, suitable for nonlinear problems with possible stiffness degradation.

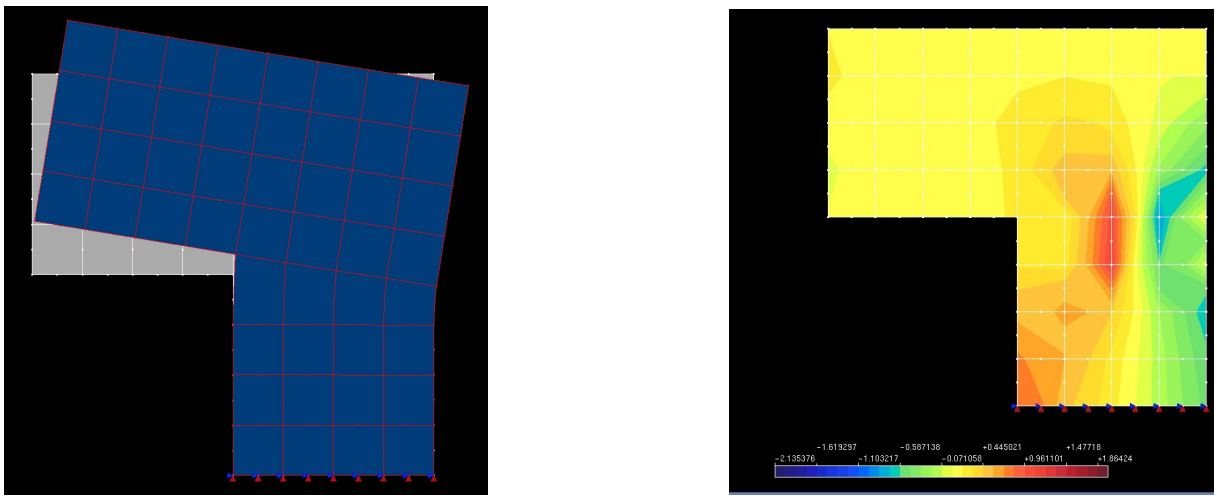
The analysis was performed using both the classical Cauchy formulation and the Cosserat continuum, allowing a comparative assessment of the responses of the two theories. The adopted solution algorithm was the standard Newton-Raphson method, with a convergence tolerance of 10^{-4}, a limit of 250 load increments, and up to 1000 iterations per increment. These numerical control parameters ensured stability of the solution even under highly nonlinear behavior.

Comparative results were evaluated based on nodal displacements, stress fields, and the evolution of the response during the nonlinear iterative process, as provided by the post-processing module of INSANE.

4 Results and Discussions

The analysis based on the Cosserat continuum formulation exhibited a higher computational cost, requiring 225.86 seconds to complete, compared to 136.06 seconds for the classical model. In terms of displacements (Figure

4a) and stress distribution (Figure 4b), the differences between the two formulations were minor. However, the Cosserat approach provides a broader range of results, which is a consequence of its higher complexity and the additional degrees of freedom associated with microrotations.



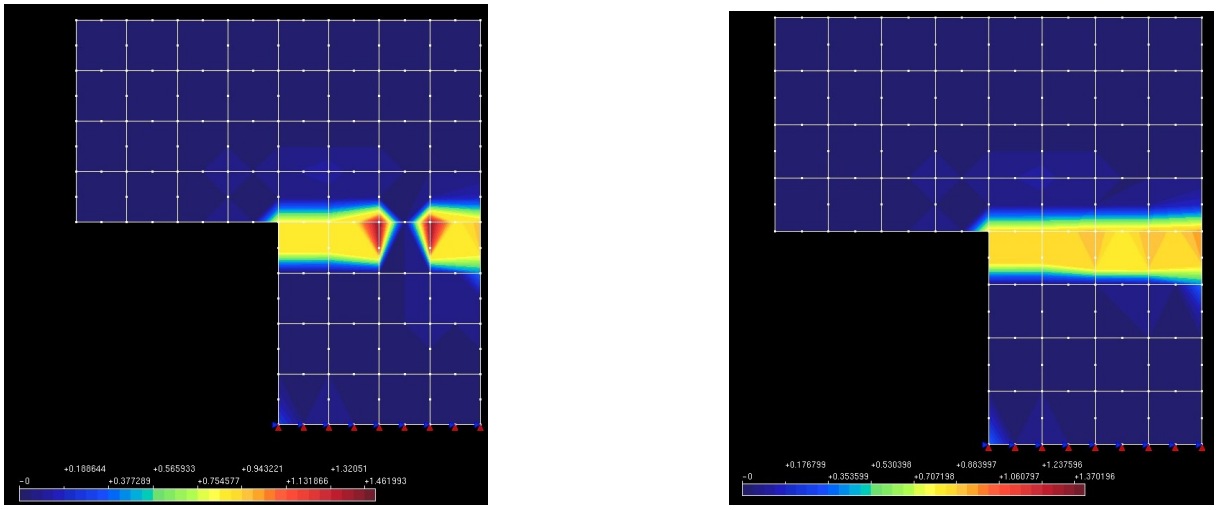
(a) Deformed configuration

(b) Stress distribution in y

Figure 4. Results for the L-shaped panel

The most significant difference was observed in the damage region. As shown in Figure 5a, the classical model exhibited a more pronounced stress concentration in the intermediate zone, while the Cosserat formulation provided a more uniform distribution (Figure 5b), especially near the rotation zone of the panel (Figure 4a). This smoothing effect is directly related to the Cosserat model's ability to represent microrotations through additional degrees of freedom, as discussed earlier.

It is also noteworthy that, in the Cauchy model, the intermediate region appears as undamaged (Figure 5a), which clearly does not reflect the physical reality considering the rotations observed, indicating a loss of accuracy in representing the phenomenon when microrotations are neglected.



(a) Damage in the classical model (Cauchy)

(b) Damage in the Cosserat model

Figure 5. Comparison of damage regions

The L-shaped panel includes experimental data regarding the displacement of the node located at the lower left edge as the load factor evolves, as reported by Winkler [14]. These data were used to validate the numerical simulations carried out in this study. Figure 6 shows that both continuum models—Cauchy and Cosserat—exhibited good agreement with the experimental results in terms of global displacements, although discrepancies were observed in the damage region.

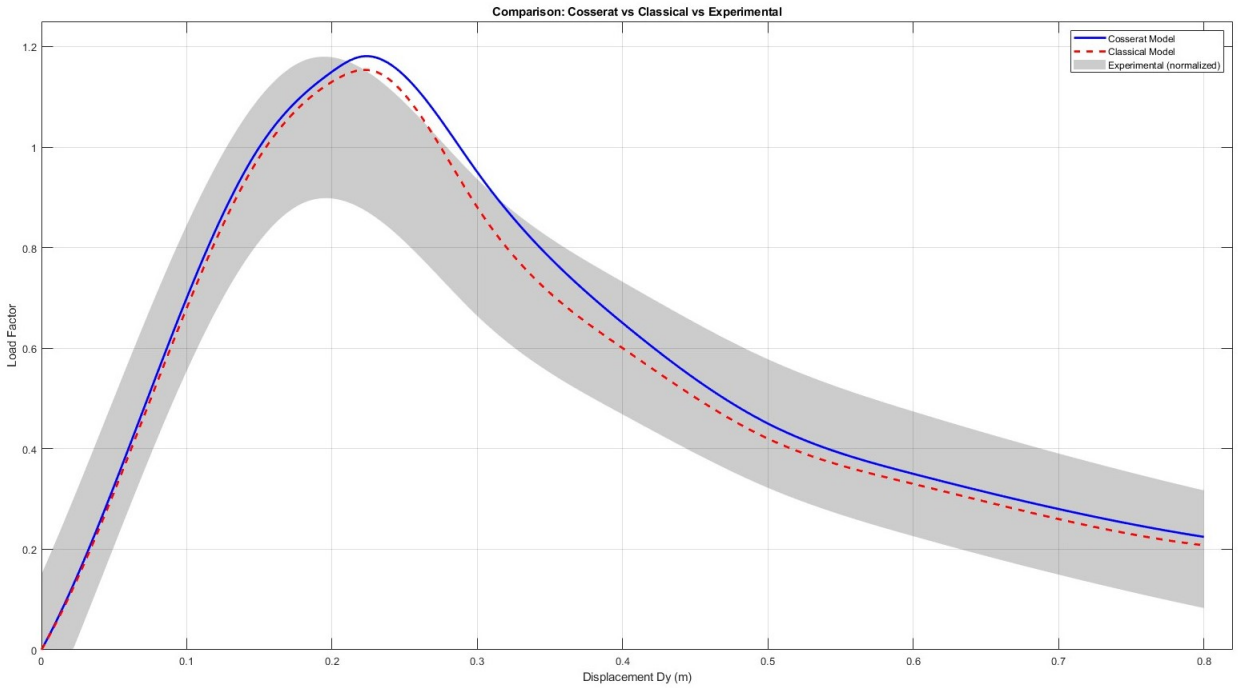


Figure 6. Comparison between experimental and numerical results: Cosserat vs. Cauchy.

5 Conclusions

This study assessed the performance of the classical Cauchy and micropolar Cosserat formulations in the nonlinear analysis of an L-shaped panel, based on numerical simulations performed with the INSANE software and experimental data available in the literature. The following conclusions can be drawn:

1. **Similar global response:** Both formulations showed good agreement with experimental displacement results, indicating the reliability of the numerical implementations for the analyzed geometry and loading conditions.
2. **Differences in damage representation:** The most significant discrepancies were observed in the damage region, where the Cauchy continuum exhibited highly localized concentrations and absence of damage in areas subjected to rotations, which does not reflect the expected physical response. The Cosserat formulation provided a smoother and more continuous damage distribution, better capturing the influence of rotations and material heterogeneity.
3. **Computational cost:** The Cosserat model required approximately 66% more processing time compared to the classical model, due to the increased number of degrees of freedom and additional complexity. This overhead should be considered when selecting the model for practical applications.
4. **Applicability:** The micropolar formulation proved advantageous in situations where rotations and microstructural effects are relevant, such as in heterogeneous materials (e.g., structural concrete, composites, or geometries with sharp discontinuities).

In summary, the use of the Cosserat continuum can represent a significant improvement in modeling phenomena not properly captured by the classical model, although at the expense of higher computational cost. Future research should address strategies to reduce this impact and investigate the model's performance in three-dimensional analyses and under different loading scenarios.

Acknowledgements. The authors gratefully acknowledge the Coordination for the Improvement of Higher Education Personnel (CAPES) for the financial support provided for the development of this research. Special thanks are also extended to the team behind the INSANE (INteractive Structural ANalysis Environment) software for offering a robust platform for advanced Finite Element Method analyses. Finally, the authors express their appreciation to the Federal University of Minas Gerais (UFMG) for the institutional support and infrastructure provided throughout this work.

Authorship statement. The authors hereby confirm that they are the sole liable persons responsible for the authorship of this work, and that all material included as part of the present paper is either the property (and authorship) of the authors.

References

[1] O. C. Zienkiewicz, K. Morgan, and K. Morgan. *Finite elements and approximation*. Courier Corporation, 2006.

[2] L. A. F. Silva. Estudo da influência da flexão e pressão externa na falha de dutos rígidos corroídos. Dissertação (mestrado em engenharia civil), Universidade Federal de Pernambuco, Recife, Brasil. Área de concentração: Estruturas. Orientadora: Silvana Maria Bastos Afonso da Silva. Coorientador: Renato de Siqueira Motta, 2025.

[3] G. Frunzio, A. Gesualdo, M. Monaco, and others. 3d fem analysis of a roman arch bridge. In *Proceedings of III International Seminar on STRUCTURAL ANALYSIS OF HISTORICAL CONSTRUCTION*, pp. 591–598, 2001.

[4] H. M. Leão and others. A critical study on phase-field modelling of fracture, 2021.

[5] R. E. Hammah, J. H. Curran, T. Yacoub, B. Corkum, and others. Stability analysis of rock slopes using the finite element method. In *Proceedings of the ISRM regional symposium EUROCK*, 2004.

[6] K. U. Katz and M. G. Katz. Cauchy's continuum. *Perspectives on science*, vol. 19, n. 4, pp. 426–452, 2011.

[7] I. Vardoulakis. Cosserat continuum mechanics. *Lecture Notes in Applied and Computational Mechanics*, vol. 87, 2019.

[8] R. Jänicke. *Micromorphic media: Interpretation by homogenisation*, 2010.

[9] A. K. Mal and S. J. Singh. Deformation of elastic solids. *(No Title)*, 1991.

[10] V. Prakash, M. M. Rahaman, and D. Roy. A microstructural defect-orientation informed phase field model. *European Journal of Mechanics-A/Solids*, vol. 109, pp. 105472, 2025.

[11] J. S. Fuina and others. Formulações de modelos constitutivos de microplanos para contínuos generalizados, 2009.

[12] Insane - interactive structural analysis environment. Acesso em: 4 ago. 2025, 2025.

[13] *Manual de Utilização do Ambiente Gráfico de Análise de Modelos Planos*. UFMG - Universidade Federal de Minas Gerais, PROPEEs - Programa de Pós-Graduação em Engenharia de Estruturas, DEES - Departamento de Engenharia de Estruturas, INSANE-Lab - Laboratório de Software Livre, Belo Horizonte, MG. Versão: 19 de setembro de 2016, 2016.

[14] B. Winkler. *Traglastuntersuchungen von unbewehrten und bewehrten Betonstrukturen auf der Grundlage eines objektiven Werkstoffgesetzes für Beton*. Innsbruck University Press, 2001.